CELL ADHESION & MIGRATION
2026, VOL. 20, NO. 1, 1–16
https://doi.org/10.1080/19336918.2026.2613628

Upregulation of LTF promotes left-sided colorectal cancer development via activating PI3K/AKT pathway

Peng Chen[a,b], Mingrui Zhang[c] and Xuefeng Bai[a]

[a]Colorectal Cancer Surgery Ward 1, Harbin Medical University Cancer Hospital, Harbin, Heilongjiang, China; [b]Department of Surgical Oncology, Chifeng Clinical Medical College Affiliated to Inner Mongolia Medical University, Chifeng, Inner Mongolia, China; [c]Department of Anesthesiology, Chifeng Clinical Medical College Affiliated to Inner Mongolia Medical University, Chifeng, Inner Mongolia, China

ABSTRACT

Lactoferrin (LTF) has gained attention as a potential anti-cancer biomarker, but its role in left-sided colon cancer (LCC) remains poorly understood. This study explores the function of LTF in LCC and its underlying mechanisms. LTF expression was significantly elevated in tumor tissues compared to normal tissues (59.67-fold increase, $p < .001$). LTF overexpression significantly enhanced LCC cell proliferation, migration, and invasion ($p < .01$), while suppressing apoptosis ($p < .05$). In contrast, LTF knockdown markedly inhibited these oncogenic behaviors. Western blot analysis demonstrated that LTF overexpression led to increased phosphorylation of PI3K and Akt proteins ($p < .01$), suggesting activation of the PI3K/AKT signaling pathway, while LTF knockdown resulted in decreased phosphorylation levels ($p < .01$). This study identifies LTF as a promoter of LCC development via activation of the PI3K/AKT pathway, suggesting LTF as a promising therapeutic target. Further research is warranted to evaluate its clinical potential in LCC treatment.

ARTICLE HISTORY
Received 26 August 2025
Revised 30 December 2025
Accepted 5 January 2026

KEYWORDS
Left-sided colon cancer; proteomics; lactoferrin; PI3K; Akt; tumor progression

Introduction

Colorectal cancer has the third highest incidence rate and the second highest mortality rate among all malignant tumors, posing a significant global health issue [1]. The left-sided colon cancer (LCC) typically refers to malignancies located from the splenic flexure to the upper rectum [2]. Compared to right-sided colorectal cancer, patients with LCC exhibit higher five-year overall survival rates [3,4]. However, the incidence of LCC is higher among younger patients; studies have shown that 65.1% of patients under 50 years old are diagnosed with LCC, compared to 47.2% of patients over 50, often resulting in a substantial impact on families [5,6]. The pathogenesis and treatment strategies for LCC differ significantly from those for right-sided colorectal cancer, highlighting the clinical importance of distinguishing between these subtypes for optimized management and treatment [7]. A retrospective study comparing the epidemiological factors and clinicopathological characteristics of patients with left-sided versus right-sided colorectal cancer indicated that patients with LCC had higher survival rate and lower recurrence rate, particularly in those with locally advanced cancer [8]. Understanding the underlying mechanisms of the development of LCC is crucial for improving patient outcomes.

Proteomics plays a critical role in identifying and characterizing functional proteins that drive the progression of malignant tumors [9]. It also aids in the discovery of biomarkers for early cancer detection and prognosis prediction, demonstrating superior performance in cancer biomarker discovery [10,11]. Increasing evidence suggests that the pronounced molecular and biological heterogeneity of cancer underscores the need for more personalized and precision-based therapeutic strategies, rather than uniform treatment approaches [12,13]. In this context, a deeper understanding of subtype-specific mechanisms, such as those underlying left-sided colon cancer, is essential for improving patient stratification and optimizing clinical management. The PI3K/AKT signaling cascade is crucial during tumor progression, which

CONTACT Xuefeng Bai 13633640048@163.com Colorectal Cancer Surgery Ward 1, Harbin Medical University Cancer Hospital, No. 150 Haping Road, Nangang District, Harbin, Heilongjiang, 150081, China
Supplemental data for this article can be accessed online at https://doi.org/10.1080/19336918.2026.2613628

participates in the regulation of cell proliferation, apoptosis, migration, invasion, tumor angiogenesis, and treatment resistance [14–16]. LTF is a potential biomarker in some types of cancers [17,18], but its role in LCC warrants comprehensive exploration.

However, the role of LTF in the development of LCC remains poorly defined. The aim of this study was to systematically investigate the expression and functional role of LTF in left-sided colon cancer using proteomic profiling and in vitro cellular assays, and to explore its potential involvement in tumor progression-related signaling pathways, thereby providing mechanistic insights into left-sided colon cancer.

Materials and methods

Sample and data collection

This study protocol was reviewed and approved by the Ethics Committee of Harbin Medical University Cancer Hospital in accordance with regulatory and ethical guidelines on 1 December 2023, approval number: CK2023106. Written informed consent of the participants was obtained before the study was conducted. Tumor and adjacent non-tumor tissues were obtained from three patients diagnosed with moderately differentiated LCC Adenocarcinoma and received laparoscopic radical LCC surgery in Department of Surgery Oncology, Capital Medical University Xuanwu Hospital Inner Mongolia Hospital (Chifeng Municipal Hospital). Patient characteristics are presented in Table S1. After surgical excision, tissue samples were immediately rinsed with ice-cold PBS, snap-frozen in liquid nitrogen within 15 minutes, and stored at −80°C until further analysis. Both groups of samples were sent to Shanghai Bioengineering Co., Ltd. for label-free quantitative proteomic sequencing.

Sequencing analysis

Protein extraction and digestion

Sodium Dodecyl Sulfate (SDS)- Dithiothreitol (DTT)-Tris (SDT) buffer (4% SDS, 100 mM Tris/HCl, pH7.6, 0.1 M DTT, catalog no. ZY2293a, ZEYE Biotechnology, Shanghai, China) was used to extracted the proteins. The Bicinchoninic Acid (BCA) protein assay kit (WB6501, Saiguo biotech, China) was applied to determine the protein concentration. Following the Filter-Aided Sample Preparation (FASP) procedure, proteins were enzymatically cleaved into peptides with trypsin (catalog no. R001100, Gibco, China) [19]. After desalting on C18 cartridges, we dried the peptides via vacuum centrifugation. Subsequently, the dried peptides were dissolved in 0.1% formic acid (FA, catalog no. Y241056, Beyotime, Wuhan, China). This study was designed as an exploratory, hypothesis-generating proteomic discovery analysis based on paired tumor and adjacent non-tumor tissues. Therefore, a formal a priori power calculation (as typically used for confirmatory randomized trials) was not performed.

SDS-PAGE

Mixed 20 μg of each sample proteins with the loading buffer (5X, catalog no. WB2001, Saiguo biotech, China). Boiled the mixture for five minutes. An SDS-PAGE gel (12.5%, catalog no. P0012A, Beyotime, Wuhan, China) was employed to separate the proteins, running at14 mA for 90 minutes. Then visualized the proteins with Coomassie Blue *R*-250.

Liquid chromatography tandem mass spectrometry (LC-MS/MS) analysis

LC-MS/MS analysis was performed using a Q Exactive mass spectrometer paired with an Easy nLC system (Proxeon Biosystems, Thermo Scientific, USA). Analysis process lasted for 60, 120, or 240 min. Add the proteins to an Acclaim PepMap100 C18-reverse phase trap column in 0.1% FA. Then separated the peptide in a mobile phase composed of 0.1% FA and 84% acetonitrile flowing at 300 nl/min. The flow rate is regulated using the IntelliFlow technology. Using a positive ion mode, the mass spectrometer utilized a data-driven top 10 strategy for selecting the precursor ion and higher-energy collisional dissociation (HCD) fragmentation. The dynamic exclusion time was 40.0 seconds. The survey scans resolution was 70, 000. The HCD spectra resolution was 17, 500.

Quantitation of the identified proteins

The MaxQuant 1.5.3.17 software was used to screen the proteins and determine the quantitation. Perform subsequent bioinformatics analysis on qualitatively and quantitatively identified proteins.

Bioinformatic analysis

Differential Analysis. Proteins with $|\log_2 FC| > 1$ and $p < .05$ (Mann-Whitney U test) were considered differentially expressed, visualized via volcano plots using the R 'limma' package.

Phosphorylated Peptides Cluster analysis. We used Java Treeview and Cluster 3.0 to conduct the Hierarchical clustering analysis. Used the Euclidean distance method to evaluate similarity, while average linkage clustering, based on the centroids of data points, was applied for grouping. Results were visualized as heatmaps with dendrograms.

Motif analysis. The MeMe tool (http://meme-suite.org/index.htm) was used for Motif identification. Peptide sequences containing the modification site, along with 6 amino acid residues upstream and 6 amino acid residues downstream (totally 13 amino acids), were extracted. These sequences were then used for motif prediction with the following parameters: width of 13, occurrences set to 20, and background specific to the species.

Subcellular localization. Protein localization was predicted using the CELLO tool (http://cello.life.nctu.edu.tw/).

Annotation of the Protein Domain. Sequence information of the proteins was analyzed through the InterProScan software to detect domain characteristics based on Pfam database (http://pfam.xfam.org/).

KEGG/GO Enrichment Analysis. To identify the homologous sequences, the sequences information of the screened protein was analyzed locally by NCBI BLAST+ and InterProScan. Assigning to the gene ontology (GO) terms, sequence annotation was performed with the Blast2GO software. Afterward, we aligned the proteins with the Kyoto Encyclopedia of Genes and Genomes (KEGG) database (https://www.kegg.jp/) to retrieve KEGG orthology identifiers (IDs). Then the IDs were utilized for pathway mapping in KEGG. With the full quantified protein dataset as the background, the Fisher's exact t test was applied the tested the enrichment analysis, applying the Benjamini-Hochberg method to adjust the *P*-values. Result was considered significant if *P*-value < .05.

Validation experiment

Cell culture

SW480 cells (LCC cell line, Qingqi Biotechnology, Shanghai, China) were cultured in RPMI-1640 medium (catalog no. 11,875,093, Gibco, China) containing 10% Fetal Bovine Serum (FBS, catalog no. FSD500, Excell Bio, China) at 37°C with 5% CO_2. Cells were divided into five groups: CON (Control), OE (LTF overexpression, transfected with LTF pc-LTF plasmid), OE_NC (negative control for LTF overexpression, transfected with pcDNA3.1 plasmid), KD (LTF knockdown, transfected with LTF siRNA), and KD_NC (negative control for LTF knockdown, transfected with scrambled siRNA).

Overexpression vector construction

To construct an overexpression plasmid for pc-LTF, the pcDNA3.1 plasmid was selected as vector. The LTF sequence was obtained from NCBI and used to construct the pc-LTF plasmid. The vector map is illustrated in Figure 1.

Cell transfection for overexpression and negative control: Mixed 125 µL Lipofectamine 3000 reagent (catalog no. L3000015, Gibco, China) with 125 µL plasmid vectors for each group and maintained at room temperature (RT) for 15 min. The pc-LTF expression plasmid and pcDNA3.1 plasmid were then added separately to the cells in the 6-well plates according to the groups for infection. RT-qPCR was used for screening and confirmation to obtain the LTF overexpressing cell line.

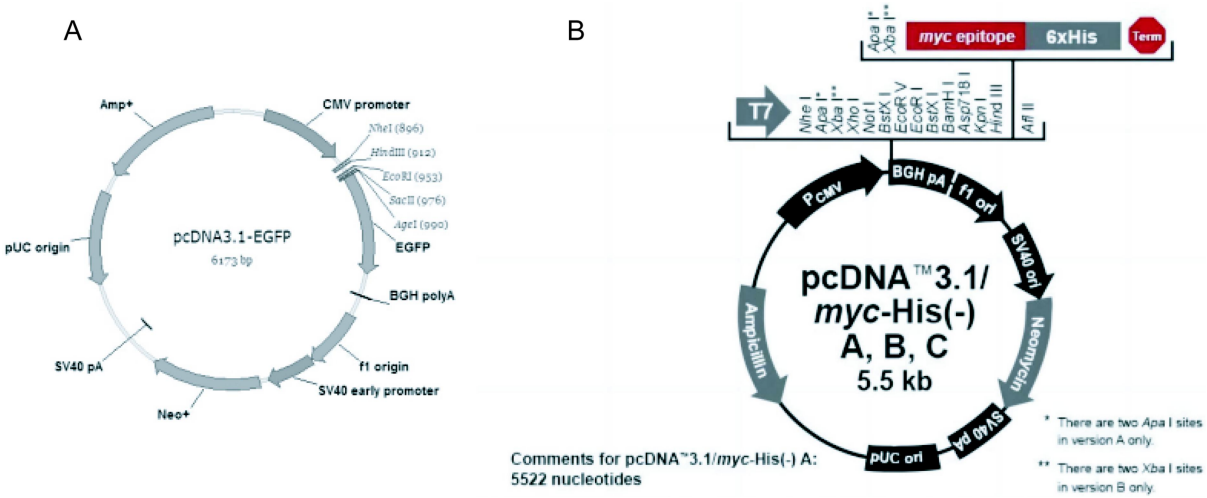

Figure 1. Schematic diagram of LTF overexpression vector construction.

To construct the LTF siRNA, the coding sequence (CDS) of the LTF gene was obtained from NCBI. Scrambled siRNA sequences were used as negative controls. For cell transfection, 20 μM siRNA duplex (2 μL), medium without FBS (200 μL) and RNAFit (10 μL) were mixed and incubated for 10 min at RT to allow the formation of the transfection complex between the double-stranded siRNA and RNAFit. Meanwhile, replaced the culture medium with 1.8 mL of pre-warmed fresh medium containing FBS. The incubated transfection complex was then added to the cells in the wells after the medium change to set the final volume per well to 2 mL and the final concentration of siRNA to 20 nM. The cells were cultured for 24 hours after transfection.

Western blot

We extracted protein from cells in the logarithmic growth phase using the phenylmethylsulfonyl fluoride (PMSF) (1 mM, catalog no. ST505, Beyotime, China)-containing radioimmunoprecipitation assay (RIPA) buffer (catalog no. P0013, Beyotime, China). Protein concentration was calculated using the BCA method, where a standard curve was plotted based on the standard protein concentrations to calculate the sample protein concentration. Separated the proteins on SDS-PAGE gel and transferred them onto a polyvinylidene fluoride (PVDF) membrane (catalog no. ISEQ00010, Millipore, Germany). Following blocking, incubated the membrane with primary antibodies at 4°C for 12 h and then with secondary antibodies at RT for 2 h sequentially. Afterward, washed the membrane using tris-buffered saline with Tween 20 (TBST) (catalog no. T1082, Saiguo biotech, China), and applied a chemiluminescent reagent mixture (catalog no. P10100, Saiguo biotech, China) to visualize the bands. After allowing the PVDF membrane to come in full contact with the reagent mixture for 3 min, it was detected using a chemiluminescent imager. Finally, Image J software (version 1.53) was utilized to analyze the optical density values and relative protein expression level was calculated. Each sample was analyzed in triplicate. The dilutions of antibodies were shown in Table 1.

Table 1. The dilution of the antibody.

Antibodies	Dilution
p-PI3K	1:1000
p-Akt	1:1000
PI3K	1:1000
Akt	1:1000
GAPDH	1:10000
Goat Anti-Rabbit antibody	1:20000
Goat Anti-Mouse antibody	1:20000

RT-qPCR

Seeded the cells into a 6-well plate and treated according to their respective groups and grown for 24 h in 37°C, 5%CO_2. RNA was extracted using Buffer RL (catalog no. BTN3070, BJBALB, China) and reverse-transcribed into cDNA using the PrimeScript RT reagent kit (catalog no. 6210A, Takara, Beijing China). The cDNA synthesis was performed using a 20 μL reaction system, and the resulting cDNA was amplified in a standard PCR machine. The cDNA was stored at −20°C. The LTF gene primer sequences are as follows: Forward: GCAACCCTTGTCCTTCCTGA (5'–3'), Reverse: GGAAGCATTTTGTGGCCTCG (5'–3'). GAPDH was used as the housekeeping gene (Forward: 5'-GGAGCGAGATCCCTCCAAAAT-3,' Reverse: 5'-GGCTGTTGTCATACTTCTCATGG-3') (Table S2). Primer specificity was confirmed via NCBI BLAST, confirming no nonspecific binding to other human genes. Relative expression was calculated using the $2^{-\Delta\Delta Ct}$ method. Each sample was analyzed in triplicate.

Cell counting kit-8 (CCK-8) assay for cell proliferation

Cells were seeded into a 96-well plate. Then incubated for 4–8 at 37°C, 5% CO_2 until the cells adhered to the plate. After adhesion, treated the cells with different concentrations of the solutions (according to the experimental groups, with six replicate wells per group) for 24 h. After treatment, added 10 μL CCK-8 (catalog no. BA00208, Bioss, China) to each well and maintained for 2 h. Then the optical density (OD) was detected at 450 nm. Each group was measured in six biological replicates, and blank controls were included to subtract background absorbance.

Flow cytometry for apoptosis detection

Treated the cells for 24 h according to the experimental groups. Collected the cells and centrifugated for 5 min at 1000 rpm. The supernatant was discarding. Cells were resuspended in 1X Annexin V Binding Solution (catalog no. C1070S, Beyotime, China). The final concentration of the cell was set to 1 × 10^6 cells/mL. Mixed the cell suspension (100 μL) with Annexin V-FITC (5 μL) and PI Solution (5 μL) (catalog no. C1062, Beyotime, China). Incubated the mixture for 15 min in the dark at RT. Afterward, added 400 μL 1X Annexin V Binding Solution. Analyzed the samples using the flow cytometry within 1 hour.

Wound healing assay

Equidistant lines, spaced 0.5 cm apart, were marked on the underside of a 6-well plate. Seeded the cells into the 6-well plate and grown to 90% confluence at 37°C, 5% CO_2. Equidistant lines (0.5 cm apart) were marked on the plate underside. A scratch was made using a 200 μL pipette tip along the marked lines. Images were captured at 0 h, 24 h, and 48 h using a microscope. The relative migration rate was calculated as (initial wound width – wound width at timepoint)/initial wound width × 100%.

Transwell assay

SW480 cells (5×10^4 in 100 uL FBS-free medium) were seeded in the upper chamber of a Transwell plate. Added 600 uL medium with 10% FBS to the lower chamber. We then incubated the cells for 24 h at 37°C, 5% CO_2. After incubation, the upper chamber was removed and observed under a microscope. The medium in the lower chamber was aspirated, and chambers were washed using PBS solution. The chambers were then placed back, washed again, and the PBS solution in the lower chamber was aspirated. Approximately 400 μL of 4% paraformaldehyde (catalog no. P0099, Beyotime, China) was placed into the lower chamber for fixation. Placed the upper chamber back on the culture plate and fixed for 10 min. After removing the upper champer, the fixation solution in the lower chamber was aspirated, and crystal violet (catalog no. V5265-250 ML, Sigma-Aldrich, USA) staining solution was used to stained the cells for 15 min. After staining, the upper chamber was washed thoroughly with water and air-dried. Observations and photographs were taken under a microscope.

Data analysis

GraphPad Prism 9 (9.4.0) and R software (4.3.3) were used to perform data analysis and visualization. Data was presented as means ± standard deviation (SD). Normality was assessed using the Shapiro-Wilk test, and homoscedasticity was tested with Bartlett's test. For proteomic data ($n = 3$), group comparisons used the Mann-

Whitney U test. For cell-based experiments ($n = 3$ or 6 biological replicates), one-way ANOVA with Tukey's post hoc test was used for normally distributed, homoscedastic data. A p-value < .05 was considered significant.

Results

Proteomic analysis reveals higher FTL expression in LCC tissues

The results of the proteomic sequencing are as follows: a total of 207,013 spectra were matched, with a total spectrum count of 651, 845; 43,409 unique peptides were identified, of which 41,715 were quantified; 4553 proteins were identified, of which 4314 were quantified (Figure 2(A)). Differential analysis using the 'limma' package identified 45 upregulated and 67 downregulated proteins. The distribution of proteins with differential expression was presented by a volcano plot (Figure 2(C)), and a heatmap of the differential protein expression allowed for clustering analysis to distinguish between LCC and normal tissues, indicating significant differences between the two (Figure 2(B)). LTF was chosen as the key protein due to its 59.67-fold expression difference in the differential analysis. A Venn diagram illustrated the common proteins between the two groups, with 261 unique proteins in the tumor tissues, 53 unique proteins in the normal tissues, and 4206 common proteins between both groups (Figure 2(D)).

GO and KEGG enrichment analyses highlight pathways involved in LCC progression

The GO term analysis demonstrated the enrichment of the proteins with different expression level in the following functional processes: biological processes (BP), including extracellular matrix organization, chondrocyte development involved in endochondral bone morphogenesis, extracellular structure organization, defense response to fungus, disruption of cells of other organism; cellular components (CC), including collagen-containing extracellular matrix, Golgi lumen, extracellular matrix, extracellular matrix component, collagen trimer; and molecular functions (MF), including extracellular matrix structural constituent, glycosaminoglycan binding, heparin binding, extracellular matrix structural constituent conferring tensile strength, collagen binding (Figure 3(A)). Pathways related to Focal adhesion, Pathways of neurodegeneration – multiple diseases, Human papillomavirus infection, ECM-receptor interaction, and PI3K-Akt signaling pathway, were significantly enriched in KEGG analysis, indicating that differentially expressed proteins were primarily related to the above pathways (Figure 3(B)).

Subcellular localization analysis indicates extracellular dominance of LTF in LCC

Using Cello software for the analysis of protein expression sub-localization, the results revealed that 135 proteins were expressed in the nuclear, 78 in the cytoplasmic, 52 in the extracellular, 32 in the plasma membrane, and 27 in the mitochondrial compartments. Furthermore, there were 6 proteins with unclear expression locations. Among these, our focus was on the LTF, which was found to be expressed in the extracellular compartment (Figure 4).

LTF enhances proliferation and inhibits apoptosis in LCC cells

To investigate the impact of LTF on proliferation and apoptosis of LCC cells, we transfected the SW480 cells with the pc-LTF plasmid (OE group), pcDNA3.1 plasmid vectors (OE_NC group), siRNA (KD group), and scrambled siRNA (KD_NC group). We then performed CCK8 and flow cytometry to test the cell viability and apoptosis. As showed in Figure 5(A), LTF gene expression in the OE group was obviously higher than that in the OE_NC group ($p < .001$). In comparison to the KD_NC groups, the KD group exhibited significantly lower LTF gene expression ($p < .001$), demonstrating the successful implementation of our transfection experiments (Figure 5(A)).

CCK8 assays showed that the cell viability in LTF KD group was obviously lower compared to the KD_NC group. Consistently, the OE group exhibited significantly higher cell viability compared to the OE_NC group (Figure 5(B)).

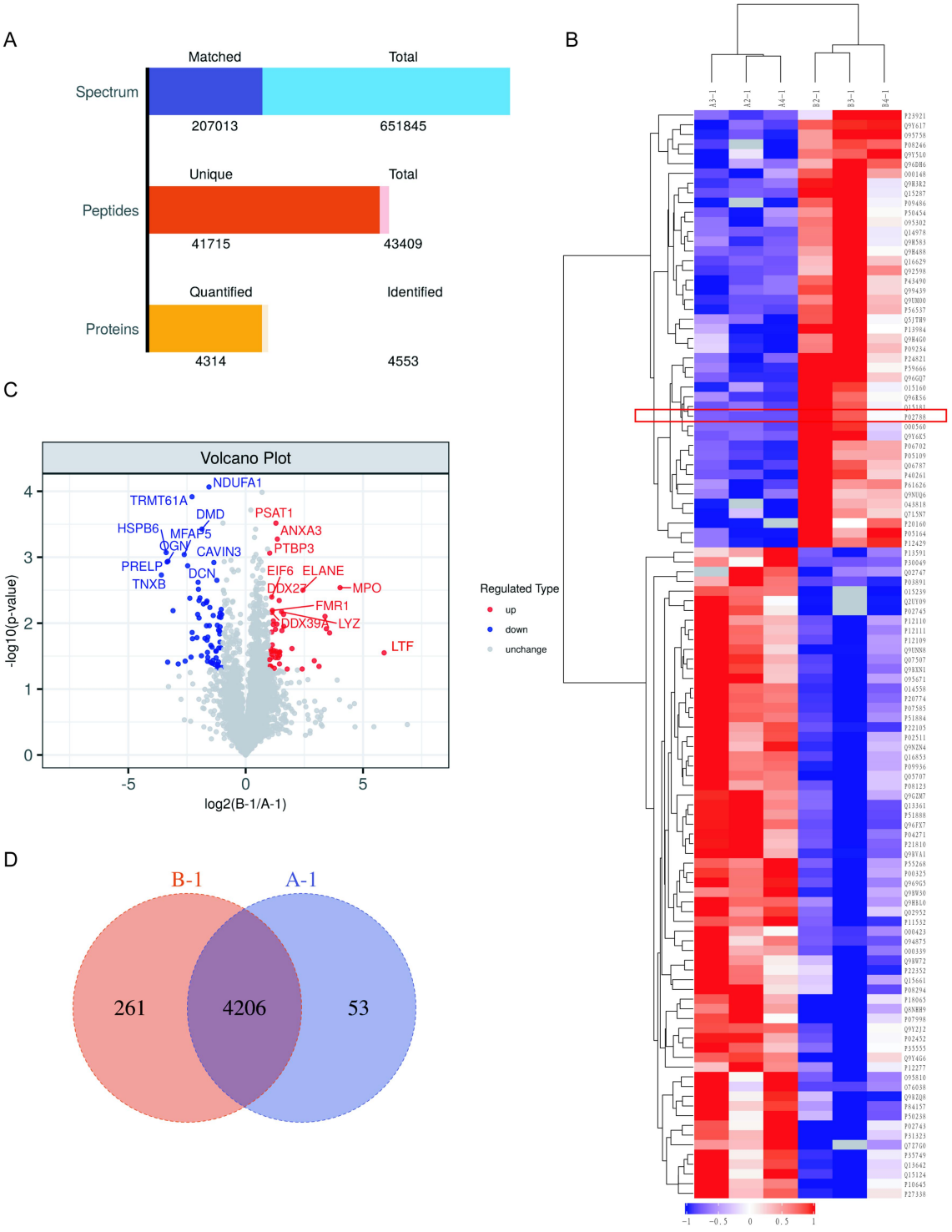

Figure 2. FTL exhibited higher expression level in LCC. A. Identification and quantification statistics, detailing the entire set of spectra, unique peptides, and proteins identified and quantified. B. Expression patterns of proteins with differential expression. Red color represents the upregulated proteins. Blue color represents the downregulated proteins. C. Volcano plot of identified proteins. Red color represents the upregulated proteins. Blue color represents the downregulated proteins. Gray color represents non-differentially expressed proteins. D. Venn diagram of differential expressed proteins. B-1, tumor tissues, A-1, adjacent tissues.

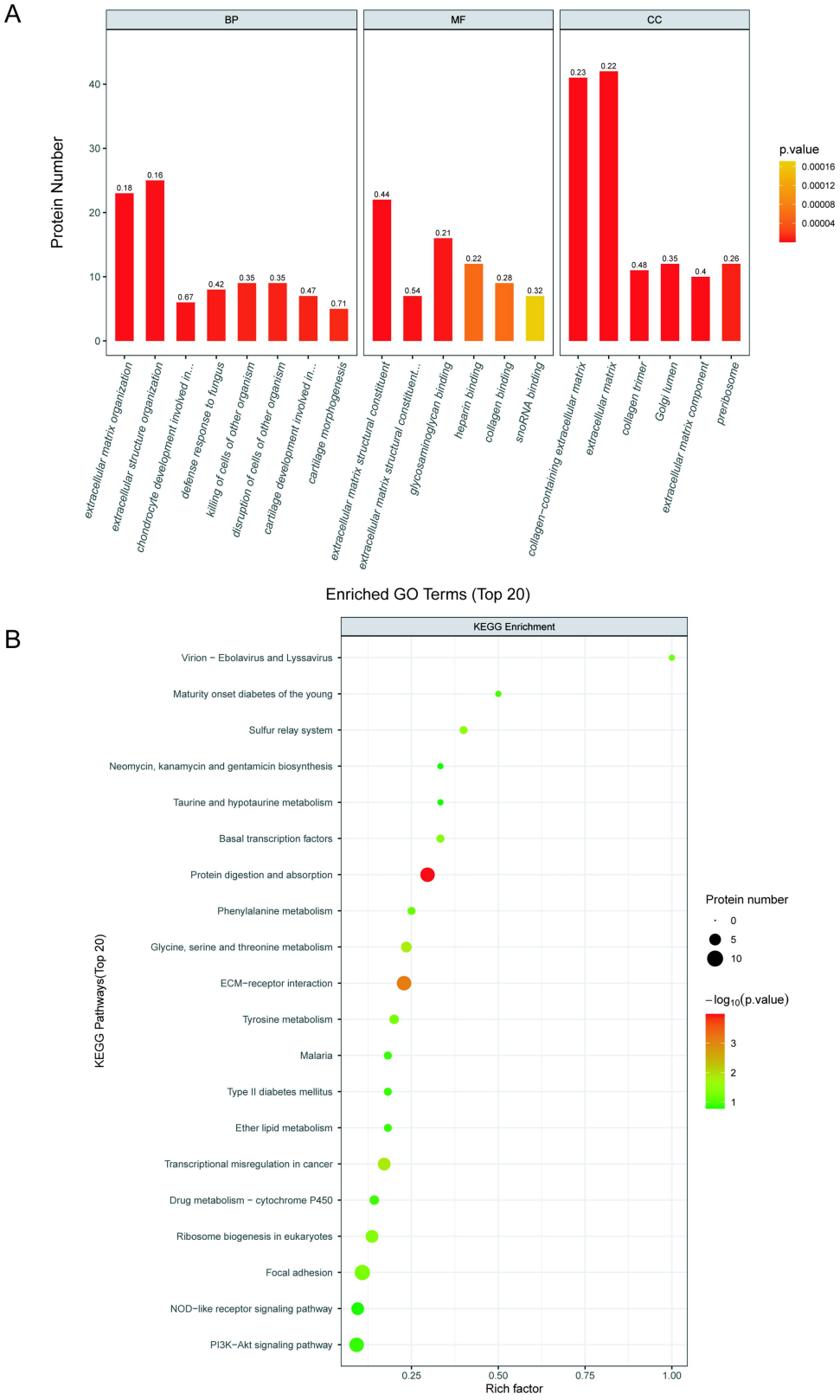

Figure 3. The KEGG pathway and GO term analysis of proteins with different expression level in LCC. A, gene Ontology (GO) enrichment analyses of differential proteins in LCC, BP bar represents the biological process, CC bar represents a cellular component, MF bar represents molecular, B, KEGG enrichment analyses of differential proteins in LCC.

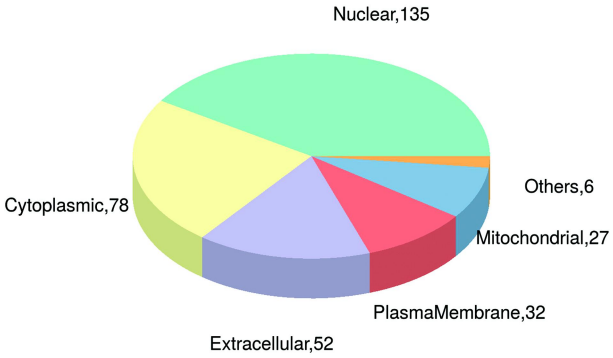

Figure 4. Results of subcellular localization analysis.

Cell apoptosis rate in the OE group was lower than that in the OE_NC group, while the cell apoptosis rate in the KD group was higher than that in the KD_NC group, indicating a significant difference (Figure 5(C)).

LTF overexpression increases cell migration and invasion in LCC

We used the wound healing and transwell assays to further verify the impact of LTF on the capacity of migration and invasion. As shown in Figure 6A, the left panel displays the cell migration status of different groups at 0 h and 24 h. The right panel represents the relative migration rate of each group. We found that, compared to the KD_NC and OE_NC groups, the migration in the KD significantly decreased, while it was obviously increased in the OE group ($p < .001$). When comparing the KD group to the KD_NC group, the relative invasion rate of the KD group was lower than that of the KD_NC group. Similarly, the relative invasive rate of the OE group was significantly higher than that of the OE _NC group, demonstrating a significant difference (Figure 6(B)) ($p < .001$).

LTF activates PI3K/AKT signaling pathway in LCC cells

As bioinformation analysis showed that PI3K-Akt signaling pathway may relate to LCC development, we further explore whether LTF expression level has an impact on the PI3K/AKT pathway via western blot. We found that p-PI3K and p-Akt expression in the OE group were significantly higher than those in the OE_NC group, while no significant differences were observed in PI3K and Akt expression. In contrast, when comparing the KD_NC group with the KD group, the p-PI3K and p-Akt protein levels in the KD group were lower than those in the KD_NC group, while no significant differences were observed in the PI3K and Akt protein levels between the two groups (Figure 7(A-B)).

Discussion

In the current research, we noted that LTF is upregulated in LCC and may be related to PI3K-Akt pathway using label-free quantitative proteomics. Then we further validated the impact of LTF on cell biological processes in vitro and demonstrated that cell proliferation, migration, and invasion was promoted, and cell apoptosis was suppressed by LTF. Western blots showed that PI3K-Akt signaling pathway was active by overexpression of LTF, which was consistent with the results of label-free quantitative proteomics. After conducting protein extraction and proteomic sequencing on three clinically collected tissue samples of left-sided colon cancer, we have identified differentially expressed proteins. We found that the LTF expression in cancer tissues is 59.67-fold higher compared to adjacent non-cancerous tissues. Numerous studies have demonstrated that LTF exhibits inhibitory effects on various cancers [20,21]. Moreover, LTF possesses immunomodulatory properties, enhancing the immune response of the body by strengthening the killing effect of natural killer cells [22] and macrophages [23]. Additionally, LTF promotes an anti-tumor immune response by regulating the secretion of cytokines. Our proteomic sequencing of clinical samples reveals a high expression of LTF in left-sided colon cancer tissues, suggesting that LTF may contribute to the

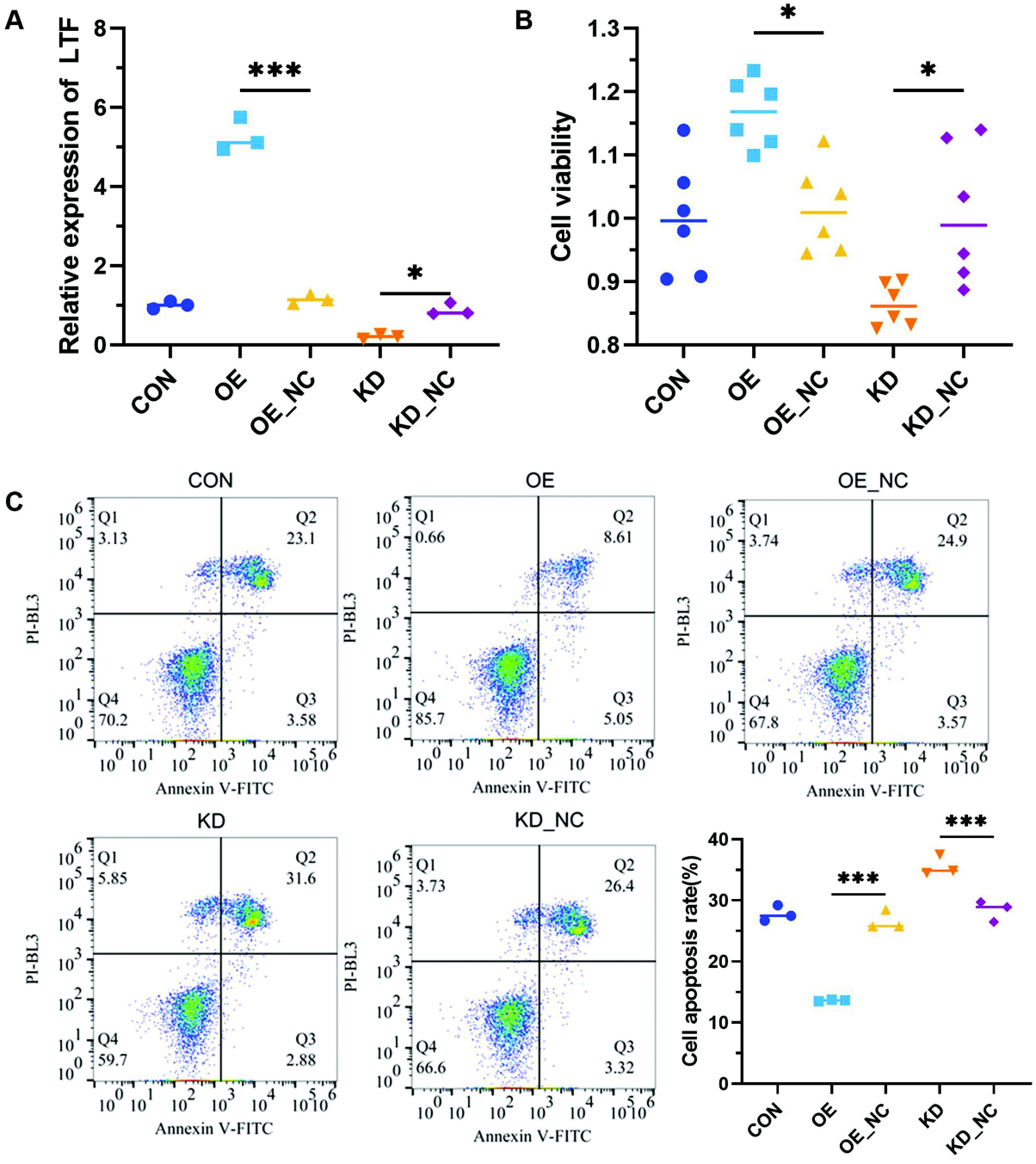

Figure 5. Effects of LTF on cellular functions. A. Relative LTF mRNA expression in the control group (CON), negative control of overexpression group (OE_NC), overexpression group (OE), scrambled siRNA group (KD_NC) and knockdown group (KD) ($n = 3$ biological replicates). B. Changes in cell viability after treatment for 24 h in different treatment groups ($n = 6$ biological replicates). C. Cell apoptosis analysis in different treatment groups using flow cytometry, demonstrating the distribution of apoptosis rates among groups ($n = 3$ biological replicates). Statistical significance determined by one-way ANOVA with Tukey's post hoc test. (*$p < .05$, ** $p < .01$, *** $p < .001$).

development of LCC. This finding aligns with the research conducted by Dong et al [21]. In healthy conditions, the concentration of LTF in the blood varies but remains relatively stable. However, during infections, inflammation, excessive iron intake, or tumor growth, the concentration of LTF increases [24,25]. This may explain why the concentration of LTF in cancer samples is obviously higher than that in non-cancerous tissues. Nevertheless, research on the role of LTF in left-sided colon cancer is relatively limited.

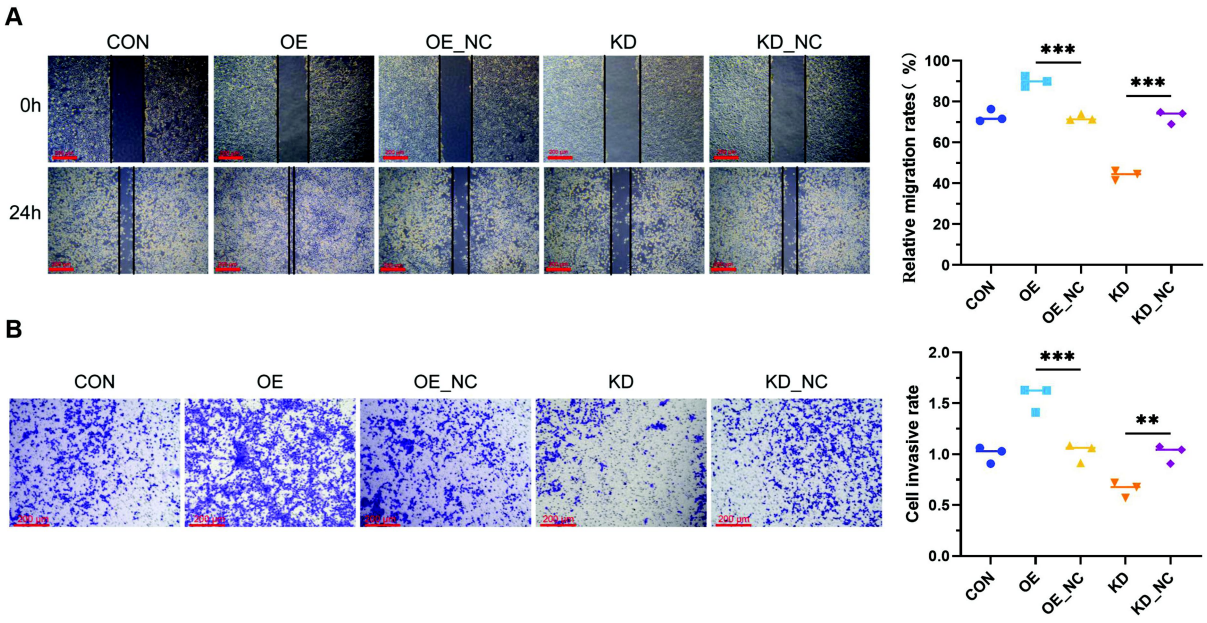

Figure 6. The impact of LTF expression on the capacity of cell migration and invasion. A. Results of the wound healing assay and quantification of relative migration rate. B. Results of the transwell assay and quantification of invasive rate. Scale bar = 200 μm. Statistical significance determined by one-way ANOVA with Tukey's post hoc test ($n = 3$ biological replicates). (**$p < .01$, *** $p < .001$).

Increasing evidence indicates that the biological roles of LTF are highly context-dependent across tumor types and experimental settings. In clear cell renal cell carcinoma, LTF downregulation is closely related to cancer malignancy, and restoring LTF expression has been reported to suppress metastatic progression, supporting a tumor-suppressive role of LTF [26]. In contrast, recent reviews have also emphasized that the biological effects of LTF are highly context-dependent and may vary across tumor subtypes, molecular backgrounds, and experimental settings. Depending on the form and source of LTF, including endogenous LTF expression and exogenous LTF supplementation, these effects can differentially influence tumor-related processes and immune regulation [27]. Therefore, our observation that LTF enhances PI3K/AKT activation in left-sided colon cancer cells likely reflects a subtype-specific regulatory pattern rather than a universal effect across malignancies.

Cell proliferation and migration are significant hallmarks of tumor progression [28,29]. We further investigated the effects of knocking down and overexpressing the LTF gene on tumor cell proliferation and migration capabilities. Our experimental demonstrated that LTF expression level significantly impacts proliferation, migration, and invasion ability, with LTF knockdown obviously suppressed proliferation, migration and invasion, while LTF overexpression significantly promoted tumor cell proliferation, migration, and invasion. Interestingly, our findings are inconsistent with previous reported by Qiu et al. [26] and Zheng et al. [30] Based on existing references, LTF exhibits anti-cancer effects, which are not only related to preventing oxidative stress and inflammation that can lead to DNA damage and tumorigenesis; but also to preventing cancer development or suppression by stimulating adaptive immune responses [31]. LTF can directly inhibit cancer cell proliferation, survival, migration, and metastasis, and accelerate cancer cell death [27,32], potentially due to its subcellular localization. LTF also binds to iron, thereby inhibiting tumor growth, and metastasis, or inducing tumor apoptosis [33]. Nevertheless, in the current study, the apoptosis rate in the LTF overexpression group was lower than that in the OE_NC group, while the apoptosis rate in the knockdown group was higher than that in the KD_NC group, indicating that LTF plays an anti-apoptotic role in LCC cell, which demonstrated that the mechanism of LTF in LCC maybe different from other tumors [34].

The PI3K/Akt pathway exhibits an obvious promoting effect in various cancers, and Its activation is often associated with rapid proliferation and enhanced anti-apoptotic capabilities of tumor cells [35,36]. Given the significant enrichment of the PI3K/Akt pathway in our KEGG enrichment analysis, we examined the

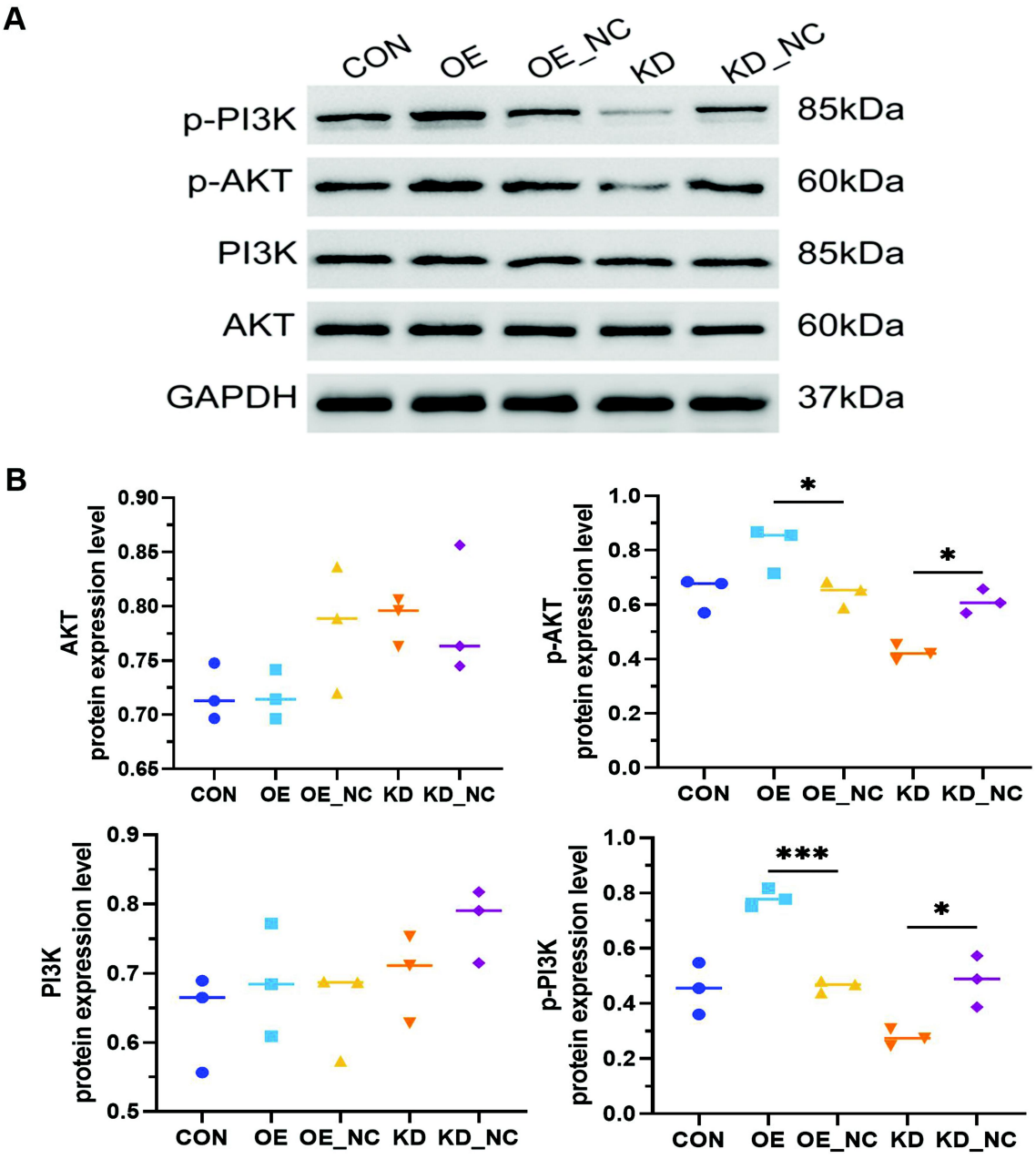

Figure 7. Impact of LTF on the PI3K-Akt pathway. A. Western blot of protein expression in different treatment groups. B. Quantitative analysis of the protein expression levels. Statistical significance determined by one-way ANOVA with Tukey's post hoc test ($n = 3$ biological replicates). (*$p < .05$, *** $p < .001$).

activation status of PI3K/Akt signaling by Western Blot upon knocking down and overexpressing LTF. Our results revealed that the overexpression increased PI3K and Akt phosphorylation, while knocking down of LTF significantly inhibited their phosphorylation levels. This suggests that LTF may interfere with the proliferation and migration of LCC cells by activating or inhibiting the PI3K/Akt signaling, which was further evidenced by the wound healing assay (Figure 6).

In colorectal cancer, oncogenic alterations such as TP53 mutations, KRAS activation, and mismatch repair deficiency are well-established drivers of tumor initiation and progression [37]. Notably, aberrant KRAS signaling has been shown to engage downstream pathways including PI3K/AKT, thereby promoting tumor cell survival and proliferation [38]. In this context, our findings that LTF enhances PI3K/AKT pathway activation suggest that LTF may act as a complementary modulator of this signaling axis, potentially enhancing pro-tumorigenic signals in LCC.

Importantly, LTF-mediated activation of PI3K/AKT may represent a KRAS-independent or cooperative mechanism, contributing to pathway activation beyond canonical oncogenic mutations. These observations highlight the potential relevance of LTF within the broader molecular landscape of colorectal cancer and underscore the need for future studies to clarify how LTF signaling intersects with KRAS status and other key genetic alterations in clinical settings. These considerations indicate important direction for future investigation, as the potential therapeutic relevance of LTF may differ among cancer subtypes and require validation through integrated molecular and clinical studies.

This study has several strengths. First, we applied label-free quantitative proteomics to human clinical samples, enabling high-throughput identification of differentially expressed proteins in LCC tissues, which has rarely been addressed previously. Second, we combined proteomics with functional validation (overexpression and knockdown) in a well-established LCC cell line, enhancing the biological relevance of our findings. However, several limitations should be acknowledged. Firstly, the proteomic analysis was performed on samples from only three patients, which may not fully represent the molecular heterogeneity of LCC. This small sample size could introduce selection bias, potentially exaggerating the observed fold-change in LTF expression. Secondly, the in vitro findings were based on a single cell line (SW480), which may limit generalizability to other LCC subtypes or in vivo contexts. The lack of animal validation further restricts translational interpretation. Thirdly, while the PI3K/AKT pathway appears activated upon LTF overexpression, the causal specificity of this relationship requires further mechanistic dissection (e.g., through pharmacological inhibition or rescue experiments). Fourthly, the absence of *in vivo* validation restricts direct extrapolation of these findings to clinical settings. Lastly, the lack of detailed genomic information, including KRAS mutation status, represents a limitation of the present study. As the proteomic analysis was performed on archived clinical specimens, comprehensive molecular profiling was not available for all cases. Consequently, the potential interaction between LTF-mediated PI3K/AKT activation and KRAS-driven oncogenic signaling could not be directly evaluated. Therefore, future studies incorporating larger patient cohorts, multiple experimental models, and in vivo approaches are warranted to further validate and extend our observations. Also, incorporating integrated proteomic and genomic analyses in larger patient cohorts will be important to further elucidate the relationship between LTF signaling and key genetic alterations in LCC.

Therefore, the current study revealed the high expression of LTF in LCC and its potential role in promoting tumor development through the PI3K/Akt signaling pathway, utilizing proteomic analysis and cellular functional experiments. From a translational perspective, the identification of LTF-associated signaling alterations in LCC highlights the importance of pathway-oriented and precision-based strategies for cancer prevention and treatment. Increasing attention has been directed toward drug- and mechanism-based therapeutic approaches that target fundamental cellular processes, including protein homeostasis and immune regulation [39]. Modulation of proteostasis-related mechanisms, such as the 20S proteasome, has been proposed as a promising strategy to interfere with tumor progression and cellular stress responses [40]. In parallel, naturally derived compounds with immunomodulatory and anticancer properties, such as hinokitiol, have attracted growing interest as sustainable and potentially prophylactic interventions [41]. In this context, if LTF is considered as a potential therapeutic or adjunctive agent in the future, practical aspects such as the mode of administration merit careful consideration, as different delivery routes, including oral supplementation or alternative systemic approaches, may differentially influence its bioavailability and biological activity. Future studies may explore whether LTF-related signaling pathways intersect with these emerging strategies and how optimal administration strategies could be tailored to specific disease contexts, thereby further expanding the translational significance of LTF in left-sided colon cancer.

Acknowledgments

The authors express their appreciation to all participants in this study.

Peng Chen: Conceptualization, Investigation, Methodology, Data curation, Formal analysis, Writing - original draft; Mingrui Zhang: Investigation, Methodology, Software; Xuefeng Bai: Conceptualization, Project administration, Supervision, Writing - review and editing.

Author contributions

CRediT: **Peng Chen:** Conceptualization, Data curation, Formal analysis, Investigation, Methodology, Writing – original draft; **Mingrui Zhang:** Investigation, Methodology, Software; **Xuefeng Bai:** Conceptualization, Project administration, Supervision, Writing – review & editing.

Disclosure statement

No potential conflict of interest was reported by the author(s).

Funding

This research did not receive any specific grant from funding agencies in the public, commercial, or not-for-profit sectors.

ORCID

Mingrui Zhang http://orcid.org/0009-0009-6669-7019
Xuefeng Bai http://orcid.org/0009-0002-5094-7051

Data availability statement

The dataset generated or analyzed in this study can be provided under reasonable request.

Ethics approval and consent to participate

The study was conducted in accordance with the Declaration of Helsinki. This study protocol was reviewed and approved by the Ethics Committee of Harbin Medical University Cancer Hospital in accordance with regulatory and ethical guidelines on 1 December 2023, approval number: CK2023106. Informed consent of the participants was obtained before the study was conducted.

List of abbreviations

AKT	protein kinase B
CRC	colorectal cancer
FC	fold change
GO	Gene Ontology
KEGG	Kyoto Encyclopedia of Genes and Genomes
LC-MS/MS	liquid chromatography-tandem mass spectrometry
LCC	left-sided colon cancer
LTF	lactoferrin
PI3K	phosphoinositide 3-kinase
PVDF	polyvinylidene fluoride
RT-qPCR	quantitative real-time polymerase chain reaction
SDS-PAGE	sodium dodecyl sulfate-polyacrylamide gel electrophoresis

References

[1] Sung H, Ferlay J, Siegel RL, et al. Global cancer statistics 2020: gLOBOCAN estimates of incidence and mortality worldwide for 36 cancers in 185 countries. CA Cancer J Clin. 2021;71(3):209–249. doi: 10.3322/caac.21660
[2] Lee GH, Malietzis G, Askari A, et al. Is right-sided colon cancer different to left-sided colorectal cancer? - A systematic review. Eur J Surg Oncol (EJSO). 2015;41(3):300–308. doi: 10.1016/j.ejso.2014.11.001
[3] Guo JN, Chen D, Deng SH, et al. Identification and quantification of immune infiltration landscape on therapy and prognosis in left- and right-sided colon cancer. Cancer Immunol Immunother. 2022;71(6):1313–1330. doi: 10.1007/s00262-021-03076-2

[4] Narayanan S, Gabriel E, Attwood K, et al. Association of clinicopathologic and molecular markers on stage-specific survival of right versus left colon cancer. Clin Colorectal Cancer. 2018;17(4):e671–e678. doi: 10.1016/j.clcc.2018.07.001
[5] Degro CE, Strozynski R, Loch FN, et al. Survival rates and prognostic factors in right- and left-sided colon cancer stage i-iv: an unselected retrospective single-center trial. Int J Colorectal Dis. 2021;36(12):2683–2696. doi: 10.1007/s00384-021-04005-6
[6] Kearney DE, Cauley CE, Aiello A, et al. Increasing incidence of left-sided colorectal cancer in the young: age is not the only factor. J Gastrointestinal Surg. 2020;24(10):2416–2422. doi: 10.1007/s11605-020-04663-x
[7] Aljama S, Lago EP, Zafra O, et al. Dichotomous colorectal cancer behaviour. Crit Rev Oncol Hematol. 2023;189:104067. doi: 10.1016/j.critrevonc.2023.104067
[8] Bourakkadi Idrissi M, El Bouhaddouti H, Mouaqit O, et al. Left-sided colon cancer and right-sided colon cancer: are they the same cancer or two different entities? Cureus. 2023;15(4):e37563. doi: 10.7759/cureus.37563
[9] Hanash S. Disease proteomics. Nature. 2003;422(6928):226–232. doi: 10.1038/nature01514
[10] Tan HT, Lee YH, Chung MC. Cancer proteomics. Mass Spectrom Rev. 2012;31(5):583–605. doi: 10.1002/mas.20356
[11] Wulfkuhle JD, Liotta LA, Petricoin EF. Proteomic applications for the early detection of cancer. Nat Rev Cancer. 2003;3(4):267–275. doi: 10.1038/nrc1043
[12] Hamdy NM, Basalious EB, El-Sisi MG, et al. Advancements in current one-size-fits-all therapies compared to future treatment innovations for better improved chemotherapeutic outcomes: a step-toward personalized medicine. Curr Med Res Opin. 2024;40(11):1943–1961. doi: 10.1080/03007995.2024.2416985
[13] Youness RA, Hassan HA, Abaza T, et al. A comprehensive insight and in silico analysis of circRNAs in hepatocellular carcinoma: a step toward ncRNA-based precision medicine. Cells. 2024;13(15):1245. doi: 10.3390/cells13151245
[14] Bahrami A, Khazaei M, Hasanzadeh M, et al. Therapeutic potential of targeting PI3K/AKT pathway in treatment of colorectal cancer: rational and progress. J Of Cellular Biochem. 2018;119(3):2460–2469. doi: 10.1002/jcb.25950
[15] Yang L, Dong Z, Li S, et al. Esm1 promotes angiogenesis in colorectal cancer by activating PI3K/Akt/mTOR pathway, thus accelerating tumor progression. Aging (Albany NY). 2023;15(8):2920–2936. doi: 10.18632/aging.204559
[16] Zhong J, Ding S, Zhang X, et al. To investigate the occurrence and development of colorectal cancer based on the PI3K/AKT/mTOR signaling pathway. Front Biosci (Landmark Ed). 2023;28(2):37. doi: 10.31083/j.fbl2802037
[17] Qiu K, Ding D, Zhang F, et al. LTF as a potential prognostic and immunological biomarker in glioblastoma. Biochem Genet. 2024;63(3):2347–2362. doi: 10.1007/s10528-024-10716-6
[18] Zhang H, Zuo L, Li J, et al. Construction of a fecal immune-related protein-based biomarker panel for colorectal cancer diagnosis: a multicenter study. Front Immunol. 2023;14:1126217. doi: 10.3389/fimmu.2023.1126217
[19] Wisniewski JR. Filter aided sample preparation - a tutorial. Anal Chim Acta. 2019;1090:23–30. doi: 10.1016/j.aca.2019.08.032
[20] Li H, Yao Q, Li C, et al. Lactoferrin inhibits the development of T2D-induced colon tumors by regulating the NT5DC3/PI3K/AKT/mTOR signaling pathway. Foods. 2022;11(24):3956. doi: 10.3390/foods11243956
[21] Dong H, Yang Y, Gao C, et al. Lactoferrin-containing immunocomplex mediates antitumor effects by resetting tumor-associated macrophages to M1 phenotype. J Immunother Cancer. 2020;8(1):e000339. doi: 10.1136/jitc-2019-000339
[22] Kuhara T, Yamauchi K, Tamura Y, et al. Oral administration of lactoferrin increases NK cell activity in mice via increased production of IL-18 and type I IFN in the small intestine. J Interferon Cytokine Res. 2006;26(7):489–499. doi: 10.1089/jir.2006.26.489
[23] Zhao H-J, Zhao X-H. Modulatory effect of the supplemented copper ion on in vitro activity of bovine lactoferrin to murine splenocytes and RAW264.7 macrophages. Biol Trace Elem Res. 2019;189(2):519–528. doi: 10.1007/s12011-018-1472-1
[24] Campione E, Lanna C, Cosio T, et al. Lactoferrin against SARS-CoV-2: in vitro and in silico evidences. Front Pharmacol. 2021;12:666600. doi: 10.3389/fphar.2021.666600
[25] Zhao X, Kruzel M, Aronowski J. Lactoferrin and hematoma detoxification after intracerebral hemorrhage. Biochem Cell Biol. 2021;99(1):97–101. doi: 10.1139/bcb-2020-0116
[26] Chiu IJ, Hsu YH, Chang JS, et al. Lactotransferrin downregulation drives the metastatic progression in clear cell renal cell carcinoma. Cancers (Basel). 2020;12(4):847. doi: 10.3390/cancers12040847
[27] Cutone A, Rosa L, Ianiro G, et al. Lactoferrin's anti-cancer properties: safety, selectivity, and wide range of action. Biomolecules. 2020;10(3):456. doi: 10.3390/biom10030456
[28] Al Shamsi H. Migration and proliferation dichotomy: a persistent random walk of cancer cells. Fractal Fract. 2023;7(4):318. doi: 10.3390/fractalfract7040318
[29] Dos Santos A, Ouellete G, Diorio C, et al. Knockdown of CKAP2 inhibits proliferation, migration, and aggregate formation in aggressive breast cancer. Cancers (Basel). 2022;14(15):3759. doi: 10.3390/cancers14153759

[30] Zheng JQ, Lin CH, Lee HH, et al. Lactotransferrin downregulation serves as a potential predictor for the therapeutic effectiveness of mTOR inhibitors in the metastatic clear cell renal cell carcinoma without PTEN mutation. Biomedicines. 2021;9(12):1896. doi: 10.3390/biomedicines9121896
[31] Bielecka M, Cichosz G, Czeczot H. Antioxidant, antimicrobial and anticarcinogenic activities of bovine milk proteins and their hydrolysates - a review. Int Dairy J. 2022;127:105208. doi: 10.1016/j.idairyj.2021.105208
[32] Zhang Y, Lima CF, Rodrigues LR. Anticancer effects of lactoferrin: underlying mechanisms and future trends in cancer therapy. Nutr Rev. 2014;72(12):763–773. doi: 10.1111/nure.12155
[33] Kazan HH, Urfali-Mamatoglu C, Gunduz U. Iron metabolism and drug resistance in cancer. Biometals. 2017;30(5):629–641. doi: 10.1007/s10534-017-0037-7
[34] Shu X, Su J, Zhao Y, et al. Regulation of HeLa cell proliferation and apoptosis by bovine lactoferrin. Cell Biochem Function. 2023;41(8):1395–1402. doi: 10.1002/cbf.3873
[35] Yu L, Wei J, Liu P. Attacking the PI3K/Akt/mTOR signaling pathway for targeted therapeutic treatment in human cancer. Semin Cancer Biol. 2022;85:69–94. doi: 10.1016/j.semcancer.2021.06.019
[36] Wang Z, Cui X, Hao G, et al. Aberrant expression of PI3K/AKT signaling is involved in apoptosis resistance of hepatocellular carcinoma. Open Life Sci. 2021;16(1):1037–1044. doi: 10.1515/biol-2021-0101
[37] Yaeger R, Chatila WK, Lipsyc MD, et al. Clinical sequencing defines the genomic landscape of metastatic colorectal cancer. Cancer Cell. 2018;33(1):125–136.e3. doi: 10.1016/j.ccell.2017.12.004
[38] Peng Z, Fang W, Wu B, et al. Targeting Smurf1 to block PDK1-Akt signaling in KRAS-mutated colorectal cancer. Nat Chem Biol. 2025;21(1):59–70. doi: 10.1038/s41589-024-01683-5
[39] Mostafa AM, Hamdy NM, Abdel-Rahman SZ, et al. Effect of vildagliptin and pravastatin combination on cholesterol efflux in adipocytes. IUBMB Life. 2016;68(7):535–543. doi: 10.1002/iub.1510
[40] Atta H, Alzahaby N, Hamdy NM, et al. New trends in synthetic drugs and natural products targeting 20S proteasomes in cancers. Bioorg Chem. 2023;133:106427. doi: 10.1016/j.bioorg.2023.106427
[41] Chiang YF, Huang KC, Chen HY, Hamdy NM, Huang TC, Chang HY, Shieh TM, Huang YJ, and Hsia SM. Hinokitiol inhibits breast cancer cells in vitro stemness-progression and self-renewal with apoptosis and autophagy modulation via the CD44/Nanog/SOX2/Oct4 pathway. Int J Mol Sci. 2024;25(7):3904. doi: 10.3390/ijms25073904